

Computational Modeling of Brain Dynamics during Repetitive Head Motions

Igor Szczyrba
School of Mathematical Sciences
University of Northern Colorado
Greeley, CO 80639, U.S.A.

Martin Burtscher
School of Electrical and Computer
Engineering, Cornell University
Ithaca, NY 14853, U.S.A.

Rafal Szczyrba
Funiosoft, LLC
Silverthorne, CO 80498, U.S.A.

Abstract *We numerically model the effects of repetitive human head motions in traumatic scenarios that are associated with severe brain injuries. Our results are based on the linear Kelvin-Voigt brain injury model, which treats the brain matter as a viscoelastic solid, and on our nonlinear generalization of that model, which emulates the gel-like character of the brain tissue. To properly compare the various traumatic scenarios, we use the BIC scale, which we developed to generalize the HIC scale to arbitrary head motions. Our simulations of the brain dynamics in sagittal and horizontal 2D cross-sections of the skull interior indicate that a repetitive reversal of traumatic head rotations can increase the severity/likelihood of brain injuries due to resonance effects.*

Keywords: brain injury modeling, resonance effects

1 Introduction

A rapid head motion can result in a severe brain injury even if the skull remains intact. The origin of such Closed Head Injury (CHI) is attributed to the brain's elasticity, which supports the propagation of shear waves. Experiments and mathematical models show that in traumatic situations, brain shear waves can create locally sufficiently high values of strain to cause either neuronal damage or vein rupturing. In particular, the three known analytic solutions¹ of the *linear* Kelvin-Voigt (K-V) PDE system describing viscoelastic solids have been used to explain the mechanisms of brain hematomas [1] and to develop the Diffuse Axonal Injury (DAI) tolerance criterion. This criterion specifies characteristics of uni-directional, rapid head rotations that are likely to cause severe axonal damage [2].

We have developed numerical methods for solving the K-V PDEs in arbitrary 2D cross-sections of the skull interior. These methods have enabled us to discover and study complicated patterns of brain matter oscillations, which the K-V CHI model predicts to appear in realistic traumatic scenarios. To better emulate the gel-like character of the brain matter, we have generalized the K-V model (and our numerical solver) to a *non-linear* (N-L) CHI model, which constitutes an 'elastic' generalization of the Navier-Stokes PDEs [3-6].

It is reasonable to expect that in certain situations a repetitive head motion will amplify the brain matter oscillations, i.e., that resonance effects increase the severity/likelihood of brain injuries. Such effects could explain, e.g., why repetitive shaking of a baby (cf. the Shaken Baby Syndrome) or a series of blows to a boxer's head sometimes results in a severe brain injury despite the fact that such traumatic scenarios should be harmless according to existing brain injury tolerance criteria. (The head accelerations characterizing these two events are far below the hundreds of m/s^2 'required' by these criteria to cause a severe brain injury.)

The well-established Head Injury Criterion (HIC), which estimates the CHI severity/likelihood during translational traumatic head motions, uses the average of the acceleration magnitude's absolute value as the

¹Analytic solutions of the K-V PDEs have only been found for three domains with circular or spherical symmetry [1].

major predicting parameter [7]. Thus, according to the HIC, an injury of comparable severity should appear if the averages of the acceleration magnitude’s absolute values are the same during repetitive, alternating head accelerations and decelerations, which periodically bring the head to rest:

- a. *without* reversing the direction of the motion, and
- b. *while* reversing the direction of the motion.

However, reversing the direction of the motion can lead to a quite different evolution of the brain matter oscillations in comparison to a uni-directional motion. In particular, it can enhance or diminish the oscillations. Therefore, using the acceleration magnitude’s *absolute* value as a predictor of brain injuries in traumatic translations should be further scrutinized. Moreover, recent research indicates that in almost fifty percent of CHI in the U.S., the predominant mechanism is rotationally induced DAI [8]. Hence, the consequences of repetitive rotational head movements should be studied as well.

We present numerical results based on the K-V and N-L CHI models, which simulate traumatic head translations and rotations according to the two scenarios described above. To exclude the dynamic consequences of the differences in physical properties between the gray and the white matter, cf. [3], we treat the brain tissue as a uniform mixture of the gray and the white matter with the shear wave velocity $c=1.5\text{m/s}$, viscosity $\mu=0.01\text{m}^2/\text{s}$, and density $\delta=1.06\times 10^3\text{kg/m}^3$. Animations of Curved Vector Field (CVF) plots, which we developed to visualize the brain dynamics [6], show the evolution of the velocity field in 2D cross-sections of the skull interior while the head moves and after the forcing stops. CVF plots are particularly useful for presenting the non-laminar flow that is characteristic for the N-L model.

2 Simulation Setup

We simulate repetitive, uni- and bi-directional head translations and rotations about various horizontal and vertical axes. We chose these types of rotational axes because the topology of the considered 2D brain cross-sections (perpendicular to the axes) is essentially different due to the presence/absence of a solid membrane (falx cerebri) separating the brain hemispheres. The horizontal axes for forward and backward head rotations, which are associated with a simple connected sagittal brain cross-section, are positioned at the brain’s center of mass, the skull’s base, the neck, and the abdomen. The vertical axes for sideways rotations, which are associated with a disconnected horizontal brain cross-section, are positioned at the brain’s center of mass, the ear, and at various distances outside the skull. Forward and backward head translations can be treated as rotations about a horizontal or vertical axis positioned at infinity, i.e., the translational solutions in the sagittal and horizontal cross-sections coincide with the ‘limits’ of the rotational solutions.

Our translational simulations are gauged by the formula: $HIC_{1000T}=\max A^{2.5}T$, where T is a subinterval (in seconds) within the time span in which the head is linearly accelerated or decelerated, A is the average of the acceleration magnitude’s absolute value (in g units) over time T , and the maximum is taken over all possible intervals T . For T ranging from a few to tens of milliseconds, HIC values equal to or exceeding 1000 are usually associated with a severe brain injury [7], although recent results imply that this limit depends on T and is significantly lower for young children, cf. the HIC_{15} and HIC_{36} limit values proposed in [9, 10].

Since there is no fully-developed brain injury tolerance criterion that can be applied to all kinds of head motions², we introduced the universal Brain Injury Criterion (BIC), which is expressed in terms of energy (power) instead of acceleration. Specifically, the BIC scale extends the HIC scale to arbitrary head motions by assuming that injuries should be similar if the maximum of the total energy exchanged between the skull and the brain along some 2D cross-section is similar. Our choice to compare the energy exchange along cross-sections leads to a good agreement with the experimental results reported in [2] with respect to the rotational DAI tolerance criterion. (Using the energy exchange over the entire brain surface as the predicting parameter for brain injuries would imply critical angular velocity values that do not match these data.)

In a reference system in which either the initial or the final head velocity is zero, our formula has the form: $BIC_{1000T}=\max(2P)^{\alpha/2}T^{1-\alpha/2}$, where the maximum is taken over time intervals T and over all cross-sections, P is the absolute value of the average power (in $g\cdot\text{m/s}$) that is exchanged between the skull and the brain per unit mass along a specific 2D brain cross-section during time T , and α is a function of the victim’s age y (in years). Based on [10], the function values are: $\alpha(y \geq 6)=2.5$, $\alpha(3)=2.54$, $\alpha(1)=2.62$, cf. [12] for details.

²The criterion proposed in [11] for arbitrary traumatic head motions, which is based on the Head Injury Power, still requires the experimental determination of six constants.

To allow for proper comparison of the results, all simulations are characterized by $BIC_{36}=1000$ corresponding to the time interval $T=0.036s$ (for translations this is equivalent to $HIC_{36}=1000$). The head is accelerated and decelerated according to triangularly shaped functions, cf. Figs. 1a and 1b describing the average $a(t)$ (positive and negative) of the tangential acceleration at the domain's boundary. Figs. 1c and 1d show the average $v(t)$ of the corresponding tangential velocity at the domain's boundary.

The uni- or bi-directional acceleration/deceleration pulses bring the head to rest at even multiples of τ . In our simulations $2\tau=T/2$, T , or $2T$. For each choice of τ , the acceleration function's slope is different but the area under/over each function, which defines the average acceleration within T , is the same for a fixed rotational axis. For a given τ , the positions of the axes determine the slopes corresponding to the value $BIC_{36}=1000$. The repetitive forcing is applied to the skull for a time period $\Gamma=4\tau$ or 8τ , i.e., in some simulations the acceleration cycles shown in Fig. 1 are repeated. The total simulation time span equals 2Γ to allow monitoring how the brain matter oscillations are damped after the head comes to the final rest.

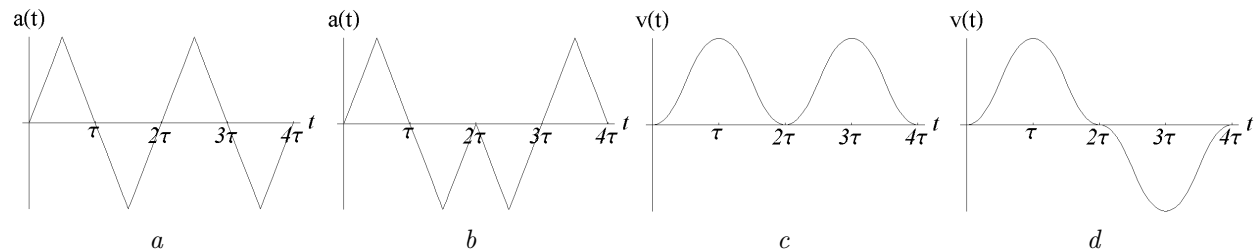


Figure 1:

Average tangential acceleration and velocity at the domain's boundary;
Uni-directional motion — panels *a* and *c*; Bi-directional motion — panels *b* and *d*.

The smooth geometry of the 2D skull-brain cross-sections is generated using cubic spline interpolations of digitized data from medical sources. For the grid size $\Delta x=10^{-3}m$, both PDE systems are numerically stable with a time step $\Delta t=10^{-5}s$. Thus, for the considered cross-sections, we use circa 35,000 grid points, and the longest simulations (with $\tau=T$) require almost 60,000 time steps. A representative selection of the 160 simulations we conducted for this study is available from the web site <http://www.funiosoft.com/brain/> in form of MPEG movies that depict the temporal evolution of the velocity field.

3 Numerical Results

Our simulations with both CHI models show that when the acceleration assumes its extrema (at odd multiples of $\tau/2$), the velocity vector field reflects the boundary conditions imposed by the skull's forcing, cf. Fig. 2 in which the dark to light shading of the curved vectors indicates the counter-clockwise direction of the brain matter motion relative to the skull.

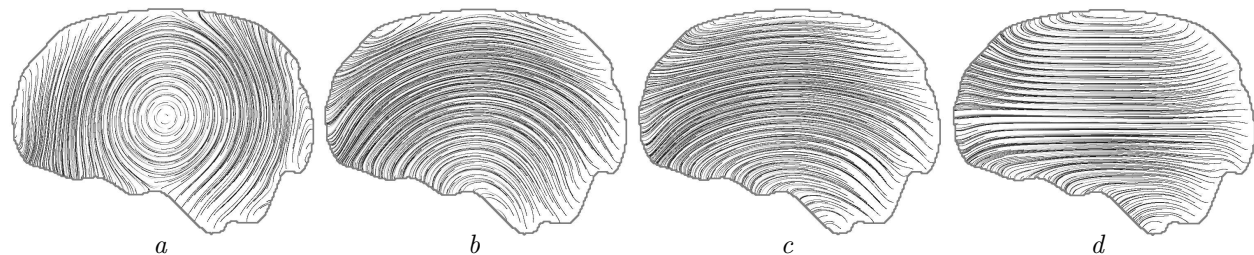


Figure 2:

K-V model: velocity field in a sagittal cross-section at $t=0.018s$ during simulations with $\tau=0.036s$ and $\Gamma=4\tau$; Panels *a*, *b*, *c* — counter-clockwise rotations about the brain's center of mass, the skull's base, and the neck, respectively; Panel *d* — forward translation.

Surprisingly, when the head comes close to the resting point, the brain matter oscillation tends to move in the *opposite* direction relative to the head's motion. In the K-V model, if the axis of rotation is within or near the skull, the oscillatory patterns mimic the brain's boundary (the skull and the falx cerebri), i.e.,

the motion has a predominantly uni-circular character within simple connected domains, cf. Figs. 3a–3c. However, if the rotational axis is moved further from the skull, in particular to infinity (translation), the oscillatory patterns become multi-circular, Fig. 3d. In the N-L model, the existence of a non-laminar flow ‘allows’ circular patterns to appear only for short impulses of forcing ($\Gamma=0.036s$), and those patterns have a uni-circular character only if the rotational axis is within the skull, cf. Figs. 4a-4d depicting a sagittal cross-section and Figs. 5a-5d showing a disconnected horizontal cross-section.

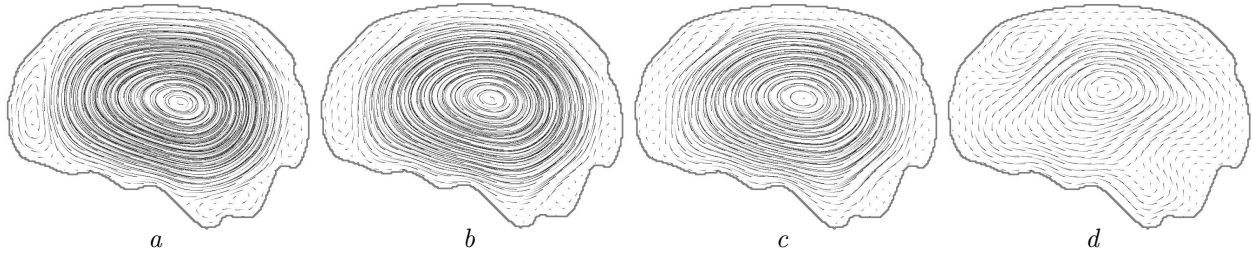


Figure 3:

K-V model: velocity field in a sagittal cross-section at $t=0.072s$ during simulations with $\tau=0.036s$ and $\Gamma=4\tau$; Panels *a*, *b*, *c* — counter-clockwise rotations about the brain’s center of mass, the skull’s base, and the neck, respectively; Panel *d* — forward translation.

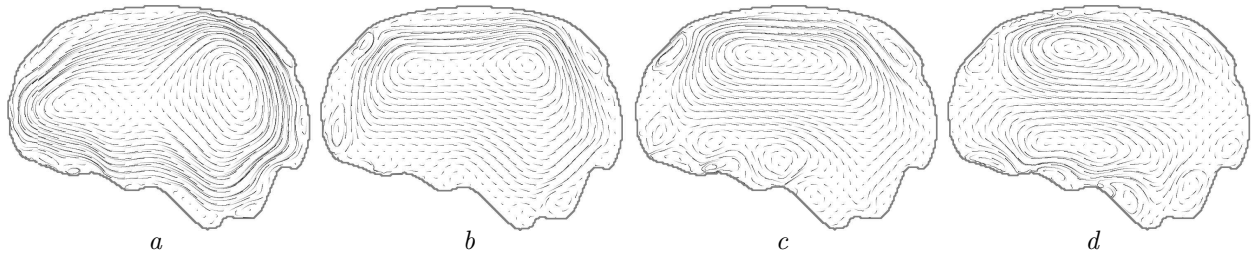


Figure 4:

N-L model: velocity field in a sagittal cross-section at $t=0.018s$ during simulations with $\tau=0.009s$ and $\Gamma=4\tau$; Panels *a*, *b*, *c* — counter-clockwise rotations about the brain’s center of mass, the skull’s base, and the neck, respectively; Panel *d* — forward translation.

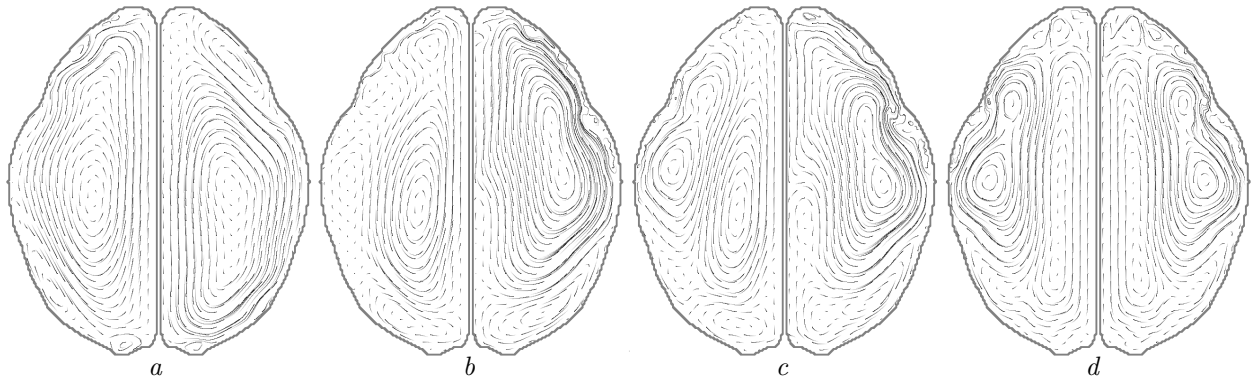


Figure 5:

N-L model: velocity field in a horizontal cross-section at $t=0.018s$ during simulations with $\tau=0.009s$ and $\Gamma=4\tau$; Panels *a*, *b*, *c* — counter-clockwise rotations about the brain’s center of mass, the ear, and twice the ear distance from the center, respectively; Panel *d* — forward translation.

The character of the oscillatory pattern appearing when the head rests is a good predictor of the resonance effect. Indeed, such effects are more likely to appear in our simulations where the head is rotated back and forth about an axis within or near the skull. The simulations also show that shorter rotational acceleration/deceleration pulses can trigger larger resonance effects than longer pulses and that the N-L case requires shorter pulses than the K-V case to obtain similar resonance effects.

Fig. 6a depicts the spatial distribution of the absolute value $\nu(t)$ of the velocity's magnitude (relative to the skull) in the sagittal cross-section when the head comes to rest at $t=2\tau=0.018\text{s}$ after a central rotation. This distribution is similar to the distribution at $t=\tau$ (when the average $v(t)$ of the tangential velocity at the domain's boundary assumes its first extremum) but has a 50% smaller maximal value $\nu_{max}(0.018\text{s})=2.5\text{m/s}$ in comparison to $\nu_{max}(0.009\text{s})=5\text{m/s}$. Fig. 6b shows that if the head is once again forced in the same direction, the maximum value of $\nu(t)$ is further suppressed 0.003s later to 1.5m/s. This is because when the rotation's direction is maintained, the counter-clockwise forcing must 'overcome' the clockwise brain matter rotation appearing at that time, and a multi-circular oscillatory pattern is created. On the other hand, if the next acceleration pulse reverses the head's rotation, the existing brain matter motion is reinforced and 0.003s later a predominantly uni-circular oscillation (as in Fig. 3a) continues with $\nu_{max}(0.021\text{s})=3\text{m/s}$, Fig. 6c.

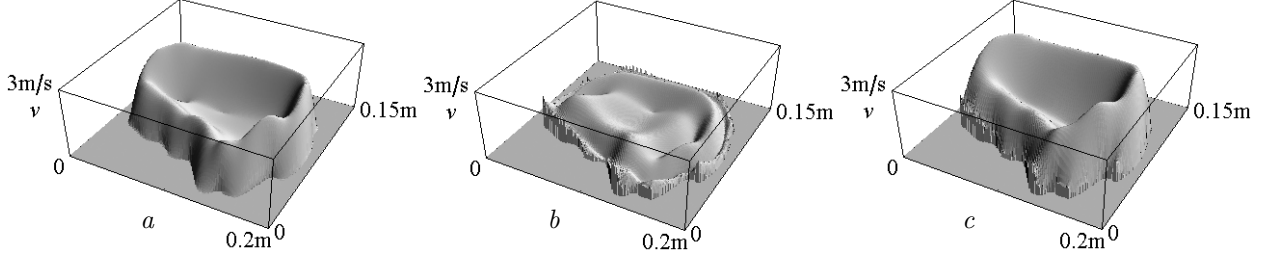


Figure 6:

K-V model: absolute value $\nu(t)$ of the velocity in a sagittal cross-section during central rotations with $\tau=0.009\text{s}$ and $\Gamma=8\tau$; Panels *a* and *b* — counter-clockwise rotation at $t=0.018\text{s}$ and $t=0.021\text{s}$, respectively; Panel *c* — counter-clockwise/clockwise rotation at $t=0.021\text{s}$.

The further evolution of these two solutions shows that when $v(t)$ again assumes its extremum at $t=0.027\text{s}$, $\nu_{max}(0.027\text{s})$ decreases to 4m/s during the uni-circular rotation, Fig. 7a, but increases to 6m/s during the bi-directional rotation, Fig. 7b, i.e., changes by $\mp 20\%$ relative to $\nu_{max}(0.009\text{s})$. Consecutive reversals of the rotational direction result in a distribution that is similar to $\nu(0.027\text{s})$ when the forcing is the largest, cf. Fig. 7c showing $\nu(t)$ at $t=0.045\text{s}$ when $v(t)$ assumes its extremum for the third time. This implies that, although repetitive bi-directional rotations do not further increase the resonance effect, high strain values can be repeatedly created in the same locations within the brain, thus enhancing the CHI severity/likelihood.

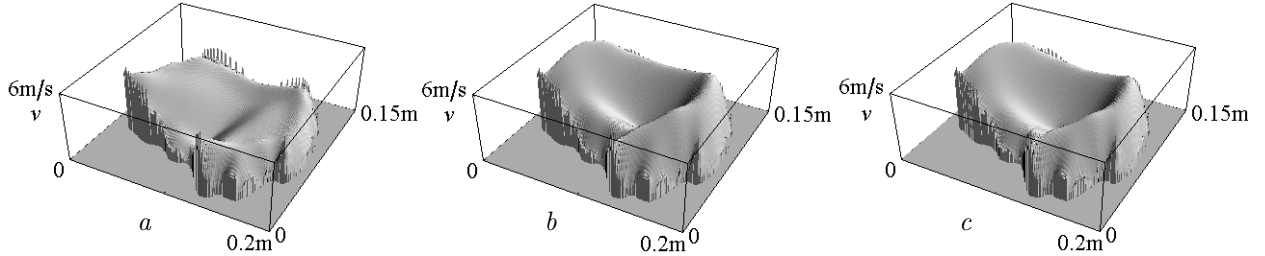


Figure 7:

K-V model: absolute value $\nu(t)$ of the velocity in a sagittal cross-section during central rotations with $\tau=0.009\text{s}$ and $\Gamma=8\tau$; Panel *a* — counter-clockwise rotation at $t=0.027\text{s}$; Panels *b* and *c* — counter-clockwise/clockwise rotation at $t=0.027\text{s}$ and $t=0.045\text{s}$, respectively.

In the disconnected horizontal cross-section, the resonance effect is larger. Indeed, in the two scenarios as above, $\nu_{max}(0.009\text{s})=2.75\text{m/s}$ decreases to $\nu_{max}(0.018\text{s})=1.9\text{m/s}$, Fig. 8a, and 0.003s later drops to 1.0m/s in the uni-directional case, Fig. 8b, but increases to 2.2m/s in the bi-directional rotation, Fig. 8c. As in the sagittal cross-section, $\nu_{max}(0.027\text{s})=1.9\text{m/s}$ in the uni-directional rotation, Fig. 9a, increases to 3.6m/s in the bi-directional case, Fig. 9b, i.e., the change in comparison to $\nu_{max}(0.009\text{s})$ is $\mp 31\%$. Again, the distributions of $\nu(t)$ are almost identical at $t=0.027\text{s}$ and $t=0.045\text{s}$ in the bi-directional case, Figs. 9b and 9c.

The resonance effects decrease when the rotational axis is moved from the center of mass. This is especially visible in the N-L case, where resonance appears only if the axis is within the skull and $\tau=0.009\text{s}$. Furthermore, no noticeable resonance occurs during head translations, cf. Figs. 10 and 11 depicting simulation results at $t=2\tau=0.072\text{s}$ and $t=0.075\text{s}$. Indeed, when the head comes to rest after a translation and then moves either back or forth, no clear uni-circular pattern emerges, Fig. 10, and $\nu_{max}(0.072\text{s})=\nu_{max}(0.075\text{s})=1.9\text{m/s}$ regardless of the motion's direction (despite that all three distributions of $\nu(t)$ are quite different), Fig. 11.

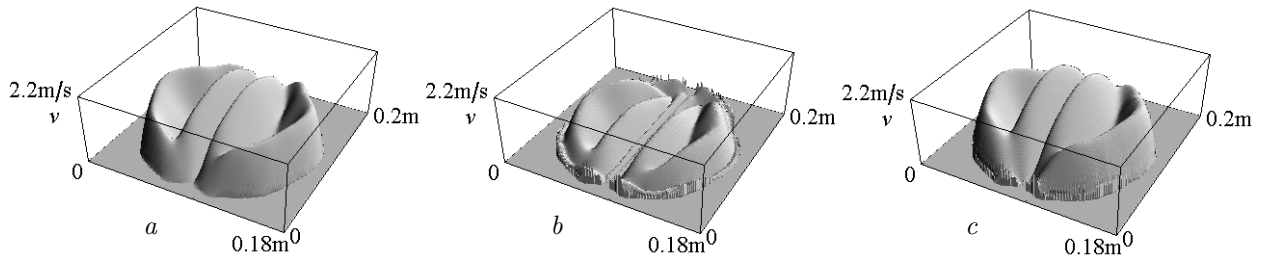


Figure 8:

K-V model: absolute value $\nu(t)$ of the velocity in a horizontal cross-section during central rotations with $\tau=0.009\text{s}$ and $\Gamma=8\tau$; Panels *a* and *b* — counter-clockwise rotation at $t=0.018\text{s}$ and $t=0.021\text{s}$, respectively; Panel *c* — counter-clockwise/clockwise rotation at $t=0.021\text{s}$.

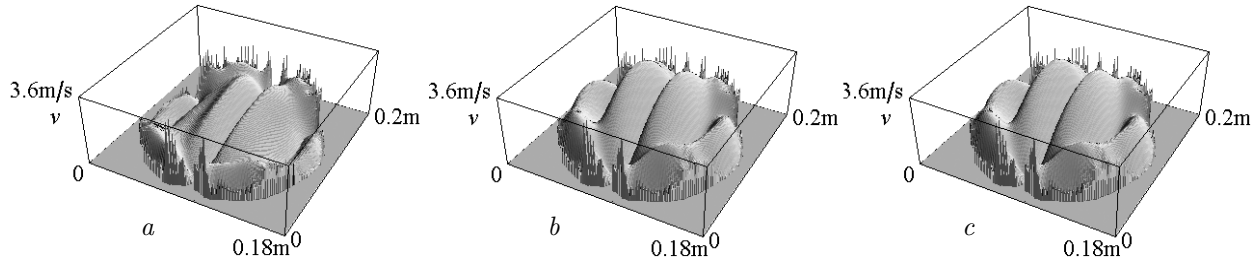


Figure 9:

K-V model: absolute value $\nu(t)$ of the velocity in a horizontal cross-section during central rotations with $\tau=0.009\text{s}$ and $\Gamma=8\tau$; Panel *a* — counter-clockwise rotation at $t=0.027\text{s}$; Panels *b* and *c* — counter-clockwise/clockwise rotations at $t=0.027\text{s}$ and $t=0.045\text{s}$, respectively.

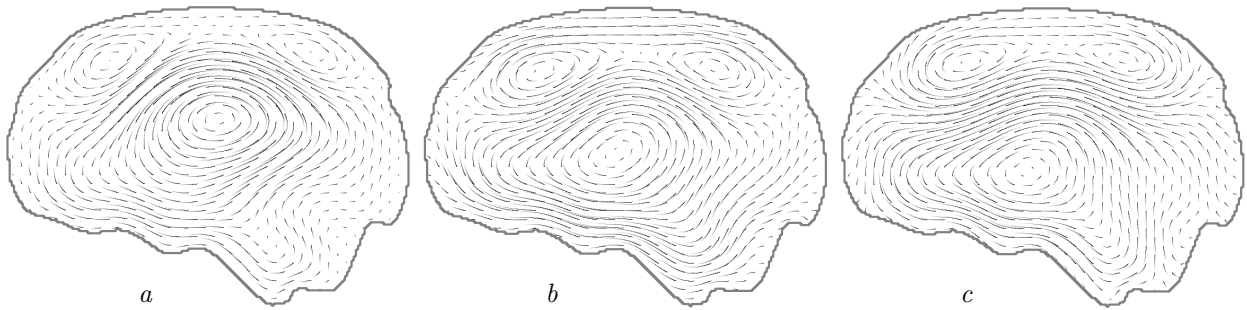


Figure 10:

K-V model: velocity field in a sagittal cross-section during translations with $\tau=0.036\text{s}$ and $\Gamma=4\tau$; Panels *a* and *b* — forward translation at $t=0.072\text{s}$ and $t=0.075\text{s}$, respectively; Panel *c* — forward/backward translation at $t=0.075\text{s}$.

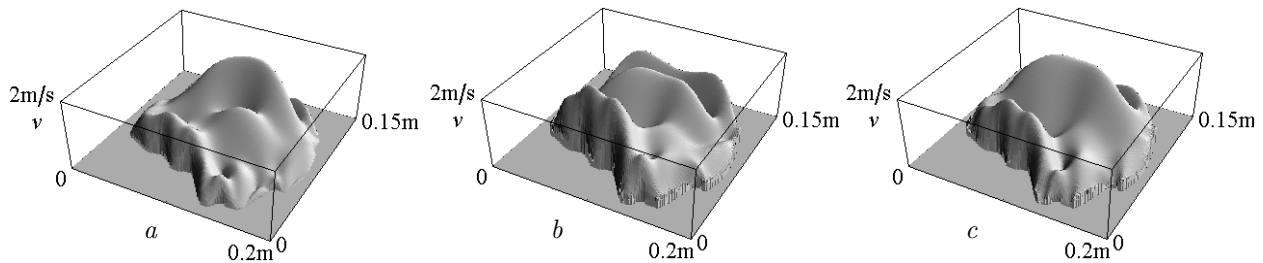


Figure 11:

K-V model: absolute value $\nu(t)$ of the velocity in a sagittal cross-section during translations with $\tau=0.036\text{s}$ and $\Gamma=4\tau$; Panels *a* and *b* — forward translation at $t=0.072\text{s}$ and $t=0.075\text{s}$, respectively; Panel *c* — forward/backward translation at $t=0.075\text{s}$.

4 Conclusions

Numerical simulations based on the linear Kelvin-Voigt CHI model and our non-linear generalization of this model predict that when a human head is close to the resting point during a repetitive rotation, the brain matter has a tendency to move in a circular way with respect to the skull and in the opposite direction of the head's motion. Consequently, changing the rotation's direction can increase the velocity induced in the brain matter relative to the skull. The observed resonance effect is more pronounced in the K-V model and in the disconnected horizontal cross-section rotated about the brain's center of mass. Shortening the period of the rotational impulses enhances the resonance effect, especially in the N-L CHI model.

During simulated head translations, no essential difference in the velocity's magnitude due to a change in the motion's direction has been observed in either CHI model. Consequently, the use of the acceleration's absolute value as the predicting parameter in the HIC formula withstands the scrutiny of our experiments. The smooth transitions of rotational solutions into translational solutions observed in all simulations support our power-based approach to generalizing the HIC scale to the BIC scale, which is applicable to arbitrary traumatic head motions. Further studies have to be performed, however, to fully validate the use of the absolute value of the energy exchanged between the skull and the brain in our BIC formula.

5 Acknowledgment

We would like to thank Intel Corporation for donating the Itanium 2 server that we used to perform part of the simulations for this paper.

References

- [1] C. Ljung. A Model for Brain Deformation due to Rotation of the Skull. *J. Biomech.*, 8:263-274, 1975.
- [2] S. S. Margulies and L. Thibault. A Proposed Tolerance Criterion for Diffuse Axonal Injury in Man. *J. Biomech.*, 25:917-923, 1992.
- [3] I. N. Szczyrba, P. K. Smolarkiewicz and C. S. Cotter, Numerical Simulations of Closed Head Injuries. *Proc. METMBS'02*, 2:486-492, CSREA Press 2002.
- [4] C. S. Cotter, P. K. Smolarkiewicz and I. N. Szczyrba, A Viscoelastic Fluid Model for Brain Injuries. *Int. J. for Numerical Methods in Fluids*, 40:303-311, 2002.
- [5] M. Burtscher and I. Szczyrba, Numerical Modeling of Brain Dynamics in Traumatic Situations – Impulsive Translations. *Proc. METMBS'05*, 1:205-211, CSREA Press 2005.
- [6] M. Burtscher and I. Szczyrba, Computational Simulation and Visualization of Traumatic Brain Injuries. *Proc. MSV'06*, 101-107, CSREA Press 2006.
- [7] J. H. McElhaney, John Paul Stapp Memorial Lecture: In Search of Head Injury Criteria. *Stapp Car Crash J.*, 49:v-xvi, 2005.
- [8] J. Meythaler *et al.*, Amantadine to Improve Neurorecovery in Traumatic Brain Injury-associated Diffuse Axonal Injury. *J. of Head Trauma and Rehabilitation*, 17:4 303-313, 2002.
- [9] M. Kleinberger *et al.* Development of Improved Injury Criteria for the Assessment of Advanced Automotive Restraint Systems. NHTSA 1998, <http://www-nrd.nhtsa.dot.gov/pdf/nrd-11/airbags/criteria.pdf>
- [10] R. Eppinger *et al.* Development of Improved Injury Criteria for the Assessment of Advanced Automotive Restraint Systems-II. NHTSA 2000, http://www-nrd.nhtsa.dot.gov/pdf/nrd-11/airbags/finalrule_all.pdf
- [11] J. A. Newman *et al.* A Proposed New Biomechanical Head Injury Assessment Function - The Maximum Power Index. *Stapp Car Crash J.*, 44:2000.
- [12] I. Szczyrba, M. Burtscher and R. Szczyrba, A Proposed New Brain Injury Tolerance Criterion based on the Exchange of Energy Between the Skull and the Brain. *Proc. of the ASME 2007 Summer Bioeng. Conf.*